UPF3A is dispensable for nonsense-mediated mRNA decay in mouse pluripotent and somatic cells

Chengyan Chen[1, #], Yanmin Shen[1, #], Luqian Li[1], Yaoxin Ren[1], Zhao-Qi Wang[3], Tangliang Li[1,2, *]

1. State Key Laboratory of Microbial Technology, Shandong University, Qingdao, China
2. School of Basic Medical Sciences, Hangzhou Normal University, Hangzhou, China
3. Leibniz Institute on Aging - Fritz Lipmann Institute, Jena, Germany

[#], These authors contributed equally.

*, Correspondence:

Dr. Tangliang Li，State Key Laboratory of Microbial Technology, Shandong University, Qingdao, China; E-mail: li.tangliang@sdu.edu.cn

Running title: UPF3A does not repress NMD in murine cells

Summary blurb

We generated a new *Upf3a* inducible knockout mouse model and showed that UPF3A does not repress expressions of NMD target genes in embryonic stem cells, somatic fibroblasts, as well as multiple tissues from adult mice.

Abstract

Nonsense-mediated mRNA decay (NMD) is a highly conserved regulatory mechanism of post-transcriptional gene expression in eukaryotic cells. NMD plays essential roles in mRNA quality and quantity control, and thus safeguards multiple biological processes including embryonic stem cell differentiation and organogenesis. UPF3A and UPF3B in vertebrate species, originated from a single *UPF3* gene in yeast, are key factors in the NMD machinery. While UPF3B is a well-recognized weak NMD-promoting factor, whether UPF3A functions in promoting or suppressing NMD is under debate. In this study, we generated a *Upf3a* conditional knockout mouse strain, and established multiple lines of embryonic stem cells and somatic cells without UPF3A. Through extensive analysis on the expressions of 33 NMD targets, we found UPF3A neither represses NMD in mouse embryonic stem cells, somatic cells, nor in major organs including the liver, spleen, and thymus. Our study reinforces that UPF3A is dispensable for NMD when UPF3B is present. Furthermore, UPF3A may weakly and selectively promote NMD in certain murine organs.

Keywords: Nonsense-mediated mRNA decay; UPF3A; Embryonic stem cell

Introduction

In eukaryotic cells, the transmission of genetic information from DNA to proteins is under stringent regulations at multiple layers. Nonsense-mediated mRNA decay (NMD) is a highly conserved gene expression regulation mechanism. NMD surveillances transcriptome quality by eliminating mRNAs containing premature termination codons (PTCs), and thus prevents accumulation of N terminal truncated protein. Meanwhile, through recognizing other NMD features, such as long 3' UTRs and 5' uORFs, NMD regulates stability of around 3-10% of normal RNA transcripts, and participates in fine-tunning gene expression (Kurosaki et al, 2019; Lykke-Andersen & Jensen, 2015). Thus, NMD plays important roles in cell fitness, stress response, etc. (Hug et al, 2016). NMD is essential for embryonic development and tissue/organ maintenance (Han et al, 2018).

UPF3A and UPF3B are unique NMD factors among all components of mammalian NMD machinery. UPF3A and UPF3B are two paralogs of Upf3 found in the baker's yeast (Lykke-Andersen et al, 2000). Phylogenetic analysis indicates UPF3A and UPF3B could be generated by a gene duplication event during the emergence of vertebrate species (Shum et al, 2016). UPF3B is a widely accepted mild NMD factor negatively regulating mRNA stability (Chan et al, 2009; Chan et al, 2007; Kunz et al, 2006; Lykke-Andersen et al, 2000). Furthermore, UPF3B participates in early and late translation termination, suggesting orchestrated roles of UPF3B in the life regulation of RNA turnover and protein synthesis (Gao & Wilkinson, 2017; Neu-Yilik et al, 2017). Interestingly, although structural and biochemical analyses show that UPF3B is one of the central factors in NMD, UPF3B loss causes very mild or even negligible NMD defects since UPF3B only regulates the stability of a small proportion of RNA targets (Huang et al, 2018a; Tarpey et al, 2007). Meanwhile, UPF3A has weak NMD-promoting activity *in vitro* (Lykke-Andersen et al, 2000);

in UPF3B deficient mammalian cells, UPF3A is considered to compensate for UPF3B loss (Chan et al, 2009; Chan et al, 2007; Wallmeroth et al, 2022; Yi et al, 2022), since UPF3A and UPF3B, through their middle domain, could bind to the MIF4GIII domain of NMD factor UPF2 (Bufton et al, 2022).

Not like other NMD factors, the knockdown of Upf3a, Upf3b or both shows no obvious developmental defects in zebrafish (Wittkopp et al, 2009). *Upf3a* or *Upf3b* knockout zebrafishes are all viable (Ma et al, 2019). In mammals, knockout mice of *Smg1*, *Upf1*, *Upf2* or *Smg6* are embryonic lethal (Han et al, 2018). *Upf3b* null mice generated by the gene trapping strategy are viable and have very mild neurological symptoms (Huang et al, 2018b). Interestingly, *Upf3a* knockout mice are early embryonic lethal (Shum et al, 2016), suggesting UPF3A may have different roles in NMD. A detailed analysis of UPF3A functions in HEK293 cells, Hela cells, mouse pluripotent cells (P19: embryonic carcinoma cell), somatic cells, and major organs, such as olfactory bulbs and testes, identified a novel function of UPF3A as a general and strong NMD repressor in mammals (Shum et al, 2016).

Recently, two back-to-back papers from Gehring's and Singh's groups revisited the NMD functions of UPF3A and UPF3B with human cell lines (Wallmeroth et al, 2022; Yi et al, 2022). Using transcriptomic data and qPCR analysis on the expressions of known NMD target genes including *RSRC2*, *SRSF2* and *ZFAS1*, Wallmeroth *et al.* found that overexpression of UPF3A or UPF3A knockdown in HEK293 cells and Hela cells does not affect NMD efficiency (Wallmeroth et al, 2022). Furthermore, NMD in UPF3B knockout cells is generally functional, and co-depletion of UPF3A and UPF3B results in stronger NMD inhibition, as revealed with RNA-Seq and qPCRs. These data indicate that UPF3 paralogs in humans are functionally redundant and could compensate for each other in NMD when one of the UPF3 paralogs is missing. Interestingly, Yi *et al.* applied human colorectal carcinoma HCT116 cell line with

a near diploid genome carrying only one UPF3B copy, and generated two independent UPF3B knockout cell lines with the CRISPR-Cas9 technology (Yi et al, 2022). They found that two UPF3B KO HCT116 cell lines showed mild NMD defects, since qPCR analysis revealed that PTC-containing isoforms of *ILK*, *NFKBIB*, *RPS9* and *SRSF3* are unregulated. The mild NMD deficiency is further supported by the finding that RNA-seq analysis showed an accumulation of PTC-containing isoforms in the transcriptome from UPF3B KO cells. Furthermore, Yi *et al.* showed knockdown of UPF3A in UPF3B KO cells further enhanced NMD inhibition. Intriguingly, UPF3A knockout HCT116 cells has a minimal effect on the abundance of PTC-containing isoforms. These two findings from Gehring's and Singh's groups reconcile a conclusion that, in human cells, UPF3A does not repress NMD, but is dispensable for NMD. Furthermore, UPF3A protein is upregulated and promotes NMD when UPF3B protein is depleted (Wallmeroth et al, 2022; Yi et al, 2022).

To briefly summarize the abovementioned findings, researches conducted with human samples strongly indicate that UPF3A is dispensable for NMD (Chan et al, 2009; Chan et al, 2007; Kunz et al, 2006; Lykke-Andersen et al, 2000; Wallmeroth et al, 2022; Yi et al, 2022), while Shum *et al.* found that UPF3A, in general, represses NMD in mouse cells and tissues (Shum et al, 2016). NMD may have species or cell type specificity. Thus, we set out to reinvestigate the UPF3A function with mouse cells and tissues. To this end, we generated a *Upf3a* conditional knockout mouse by introducing two loxP sites floxing *Upf3a* exon 3, which is identical to the published *Upf3a* conditional gene targeting strategy (Shum et al, 2016). We produced a panel of *Upf3a* deficient embryonic stem cells (ESCs), somatic cells, and tissues. To our surprise, with extensive qPCR and semi-quantitative RT-PCR analysis on the expressions of more than 30 NMD targets in embryonic stem cells, somatic cells, as well as various tissues including liver, spleen, and thymus, we found that *Upf3a*

deficiency does not cause changes on the expressions of NMD targets in these mouse cells and tissues, thus UPF3A does not play a role as a NMD repressor. Our results reinforce the conclusion that UPF3A is dispensable for mammalian NMD when UPF3B exists (Wallmeroth et al, 2022; Yi et al, 2022).

Results

Characterizing an antibody capable to detect mouse endogenous UPF3A and UPF3B proteins

Prior to our analysis on UPF3A's function in NMD, we validated a commercial antibody (Abcam 269998) that is claimed to detect UPF3A and UPF3B simultaneously in a single blot. First, we cloned mouse *Upf3a* and Upf3b cDNAs into the pEGFP-C1-EF1A vector (Li et al, 2015), and conducted western blot with protein samples isolated from U2OS cells transiently transfected with GFP empty vector, GFP-mUpf3a, or GFP-mUpf3b constructs. We could detect specific protein bands approximately at sizes of predicted GFP-mUpf3a and GFP-mUpf3b in protein lysates from U2OS cells transfected with GFP-mUpf3a and GFP-mUpf3b, respectively (Supp Fig 1A and 1B), indicating that this Abcam UPF3A+UPF3B antibody could be used to detect GFP tagged mouse UPF3A and UPF3B proteins.

To further investigate whether this antibody is capable to detect endogenous UPF3A and UPF3B, we used siRNA to knock down endogenous UPF3A and UPF3B in mouse embryonic stem cells. Through western blot, we found in control samples (untreated, reagent treated, and non-targeting siRNA treated samples), hybridization of the Abcam UPF3A+UPF3B antibody revealed two distinct bands between 52 and 66 KD. siRNA-Upf3b treated samples exhibited diminishment of the upper bands, and resulted in the great induction of lower bands (Supp Fig 1C). This finding strongly suggested that the upper band corresponds to UPF3B and the lower band represents UPF3A, since previously studies all showed that UPF3B depletion by gene knockout or knockdown strategies could dramatically increase UPF3A protein level (Chan et al, 2009; Shum et al, 2016; Wallmeroth et al, 2022; Yi et al, 2022). The fact that the lower band corresponds to UPF3A is further supported by the western blot analysis on ESCs treatment with three Upf3a siRNAs. We found in siRNA-

Upf3a treated ESC samples, UPF3A (lower band) are all mildly decreased. Thus, Abcam UPF3A+UPF3B antibody is reliable in detecting endogenous mouse UPF3A and UPF3B proteins.

UPF3A is dispensable for NMD in mouse embryonic stem cells

To override the embryonic lethality of *Upf3a* null (Shum et al, 2016), we generated a *Upf3a* conditional knockout mouse (*Upf3a*$^{flox/flox}$: *Upf3a*$^{f/f}$) with CRISPR-Cas9 technology (see "materials and methods" for details, Fig 1A) and crossed *Upf3a*$^{f/f}$ mouse with Cre-ER^{T2+} mouse, an inducible Cre transgenic line (Fig 1B). Through intercrossing *Upf3a*$^{f/f}$ Cre-ER^{T2+} mouse with *Upf3a*$^{f/f}$ mouse, we isolated E3.5 blastocysts and established several *Upf3a* inducible deletion ESC lines. Four female ESC lines showing the typical ESC morphology were selected for further analysis. We treated these ESC lines with 4-OHT for 5 days, and confirmed *Upf3a* exon 3 is completely deleted with normal genotyping and qPCR (Fig 1C, Fig 2A). Interestingly, qPCR with primer pairs specifically detecting exons 1-2, exons 7-8 or exons 8-9 showed that 4-OHT treated ESCs have around 80% reduced mRNA levels of *Upf3a*, which could be caused by an efficient NMD of truncated *Upf3a* mRNAs since *Upf3a* exon 3 deletion will generate a PTC (Supp Fig 2).

To further substantiate the successful establishment of UPF3A KO ESCs, we conducted western blot with aforementioned UPF3A+UPF3B antibody and found UPF3A proteins are completely absent in 4-OHT treatment *Upf3a*$^{f/f}$ Cre-ER^{T2+} ESC lines, indicating *Upf3a* knockout ESC lines (designated as *Upf3a*$^{\triangle/\triangle}$ ESCs or UPF3A KO mESCs) are established (Fig 1D, Supp Fig 3A). UPF3A KO mESCs are all viable and proliferative normally (Fig 1E, Supp Fig 3B). They show no phenotypic difference with their parental clones (Fig 1E, left panel).

To investigate UPF3A's role in NMD, we conducted qPCR analysis on mRNA transcripts from the following sets of NMD target genes (The features of

NMD targets selected for this study are summarized in Supp Fig 4): Genes including *Cdh11*, *Ire1*, *Smad5*, *Smad7*, *Gas5* and *Snord22* were previously used to characterize UPF3A as a NMD repressor in mouse (Shum et al, 2016); Genes including *Atf4*, *Ddit3*, *1810032O08Rik*, *Smg5*, *Smg6*, *Auf1* (PTC specific), *Hnrnpl* (PTC specific) were widely used or validated as NMD targets in mice (Li et al, 2015; Weischenfeldt et al, 2008; Weischenfeldt et al, 2012); *Eif4a2* (PTC specific) was recently identified in *Smg5*, *Smg6* and *Smg7* knockout ESCs generated with the CRISPR-Cas9 technology (Huth et al, 2022); *Upf3b*, *Smg7*, *Eif4a1* (PTC specific), *Mettl23* (PTC specific), *Sfrs10* (PTC specific), *Snrpb* (PTC specific), *Hnrnpa2b1* (PTC specific), *Luc7l* (PTC specific), and *Pkm2* (PTC specific) are designed in the current study. In our analysis, previously generated *Smg6* knockout (KO) ESC was used as a positive control of NMD inhibition (Li et al, 2015) (Supp Fig 5A, 6A). In contrast with strong increases of NMD target transcripts in *Smg6* KO ESCs (Supp Fig 5A, 6A), *Upf3a* KO ESCs showed no obvious difference in transcript levels of all NMD target genes tested (Fig 2A, and Supp Fig 6B). Furthermore, we conducted RT-PCR analysis on AS-NMD generated PTC$^+$ transcripts accumulation in *Upf3a* KO ESCs. We found a strong enrichment of PTC$^+$ isoforms in *Smg6* KO ESCs, but no difference was detected between control and *Upf3a* KO ESCs (Fig 3A-B). Thus, UPF3A is dispensable for NMD in mouse embryonic stem cells when UPF3B is present.

Knockdown of UPF3B in UPF3A deficient ESCs inhibits NMD

In human cells, UPF3A and UPF3B could compensate for each other in NMD when one of the paralogs is depleted (Chan et al, 2009; Wallmeroth et al, 2022; Yi et al, 2022). To test this hypothesis in mouse cells, we used siRNAs to knockdown *Upf3b* in our control and *Upf3a* KO ESCs. Semi-quantitative RT-PCR showed that, in control ESCs, knockdown of *Upf3b* has almost no effect

on expressions of the PTC$^+$ isoforms of *Hnrnpa2b1*, *Luc7l*, *Pkm2*, *Ptbp2*, *Flot1*, and *Sf1* (Supp Fig 7). In *Upf3a* KO ESCs, depletion of UPF3B causes a prominent increasement of PTC$^+$ isoforms of these genes. Thus, in mice, UPF3B is responsible for efficient NMD when UPF3A is lost.

UPF3A is dispensable for NMD in mouse somatic cells

To rule out a possible role of pluripotency on NMD activity, we generated somatic cell lines derived from rib tissues of 4 male *Upf3a*$^{f/f}$ Cre-ER^{T2+} mice. In this study, we named these cell lines as RDSCs (Rib muscle derived somatic cells). qPCR and western blot analysis showed that five days of 4-OHT treatment successfully depleted UPF3A in RDSCs (Fig1C, lower panel; Fig 1D; Fig 2B; Supp Fig 3A). Loss of UPF3A does not cause visible cell viability changes (Fig 1E, right panel). We then used qPCR and analyzed expressions of NMD target gene transcripts in control and *Upf3a* KO RDSCs. Previously established *Smg6* KO fibroblast was used as a positive control of NMD inhibition in somatic cells (Supp Fig 5B, 6A) (Li et al, 2015). We found *Upf3a* KO RDSCs, as compared with their parent cell lines, showed no obvious difference in transcript levels of all NMD target genes tested (Fig 2B, Supp Fig 6B). Furthermore, RT-PCR analysis on PTC$^+$ isoforms showed *Smg6* KO fibroblasts had a strong accumulation of PTC$^+$ isoforms. However, *Upf3a* KO did not result in any detectable change in the PTC$^+$ isoforms tested (Fig 3C-D). Thus, in mouse somatic cells, such as fibroblasts generated from rib muscles, UPF3A is dispensable for NMD when UPF3B is present.

UPF3A is dispensable for NMD in murine tissues

Since NMD may have tissue and cell type specificity, to expand our analysis to other cell types, we utilized *Upf3a* inducible knockout mice (*Upf3a*$^{f/f}$ Cre-ER^{T2+} mice) and treated them with tamoxifen to induce UPF3A deletion.

After another 3 weeks, PCR analysis and western blot show that UPF3A is efficiently deleted in the liver, kidney and hematopoietic system, including the spleen, thymus and peripheral blood cells from *Upf3a*$^{f/f}$ Cre-ER^{T2+} mice treated with tamoxifen (Supp Fig 8A-B). These mice are viable and have no visible behavior changes as compared with control animals (*Upf3a*$^{f/f}$ Cre-ER^{T2-} mice with Tamoxifen injection) (Data not shown). We isolated RNAs from livers, spleens, and thymus and used qPCR to determine NMD activity in samples from 4 controls (*Upf3a*$^{f/f}$ Cre-ER^{T2-} mice with TAM injection) and 4 *Upf3a* KO mice (*Upf3a*$^{f/f}$ Cre-ER^{T2+} mice treated with TAM) (Fig 2C-E, Supp Fig 6C). In general, expressions of these NMD targets show no or minimal variances between controls and UPF3A KO samples. In *Upf3a* KO livers, RNA transcripts of well-conserved NMD targets, such as *Atf4*, *Snord22*, *Snhg12*, *1810032O08Rik* and *Hnrnpl*, are mildly but all significantly upregulated, while other gene transcripts, such as *Gas5*, *Auf1*, and *Eif4a2* have a trend of increasement (Fig 2C). In *Upf3a* KO thymuses, only transcripts of *Auf1* are significantly increased, while transcripts of *Smad5*, *Gas5*, *Snord22*, *Hnrnpl*, *Ddit3*, and *Eif4a1* trend to accumulate (Fig 2D). It is interesting to note, in *Upf3a* KO livers and thymuses, none of the genes tested shows reduction at the transcript level (Fig 2C-D). Of note, the expressions of several NMD target genes, such as Smad5 and Cdh11 in livers, Smad7, Snhg12 and Mettl23 in thymuses, could not be quantified due to the technical reason that melting curves of PCR amplicons showed multiple peaks.

In Upf3a KO spleens, expression of Cdh11 is significantly upregulated, while UPR factors, including *Atf4 and Ddit3*, are significantly downregulated. Expression levels of other 16 NMD targets have no difference between the control and *Upf3a* KO samples. Overall, in spleens, UPF3A does not repress NMD (Fig 2E).

Next, we conducted RT-PCR analysis on AS-NMD generated PTC$^+$ transcripts accumulation in *Upf3a* KO livers and spleens, we found no obvious change in PTC$^+$ isoforms expression between control and *Upf3a* KO samples (Supp Fig 9).

Discussion

UPF3 is widely considered as one of the core factors of NMD machinery, which is a highly conserved mRNA surveillance mechanism in eukaryotes cells (Hug et al, 2016; Kunz et al, 2006; Lykke-Andersen et al, 2000; Lykke-Andersen & Jensen, 2015; Yi et al, 2021). In yeasts and worms, only one *Upf3* locus is identified (Hug et al, 2016). In vertebrate animals, two paralogs of UPF3, i.e., UPF3A and UPF3B exist (Lykke-Andersen et al, 2000; Serin et al, 2001). It is even more intriguing that *the Upf3b* gene is localized on the X chromosomes in mice and humans. Interestingly, although knockouts or knockdowns of NMD factors, such as *Upf1*, *Upf2*, *Smg1*, *Smg5*, *Smg6* and *Smg7*, in various types of cells manifest strong NMD defects (Huth et al, 2022; Li et al, 2015), *Upf3b* knockdowns or knockouts have mild or even negligible effects on NMD (Chan et al, 2007; Huang et al, 2011; Lykke-Andersen et al, 2000). Through generating a conditional knockout mouse model of *Upf3a* with a traditional gene targeting strategy, Shum et al. found UPF3A represses NMD in mouse pluripotent cells (P19 embryonic carcinoma cell), tissue-specific stem cells (neural stem cells and olfactory sensory neuronal precursors), somatic cells (mouse embryonic fibroblasts and neurons) as well as human 293T cells. NMD targets, such as *Cdh11*, *Smad5* and *Smad7*, are all downregulated upon *Upf3a* knockdown (Shum et al, 2016). Meanwhile, mRNAs transcripts of *Atf4*, *Gas5* and *Snord22* showed tissue-specific NMD activation or repression upon *Upf3a* knockdown (Shum et al, 2016). Due to the strong NMD repression upon *Upf3a* deficiency, Shum et al. found *Upf3a* KO mice are embryonic lethal.

Two recent studies revisited the function of UPF3A in humans (Wallmeroth et al, 2022; Yi et al, 2022). Wallmeroth et al. used the human HEK293 and Hela cell lines and found UPF3A overexpression or knockout does not affect NMD efficiency. Furthermore, Yi *et al.* utilized the human HCT116 cell line and found that UPF3A functions as a weak NMD activator (Yi et al,

2022). UPF3A could compensate for UPF3B loss and function in NMD activation since UPF3A and UPF3B double knockout cells have profound NMD defects (Wallmeroth et al, 2022; Yi et al, 2022). These two new findings, together with most of previous results, strongly indicated that UPF3A and UPF3B are mainly weak NMD activators and function redundantly in the human NMD (Chan et al, 2009; Chan et al, 2007; Kunz et al, 2006; Lykke-Andersen et al, 2000). In the discussion parts from these two studies, the authors raised several possibilities on the discrepant UPF3A's roles in the mammalian NMD: 1) UPF3A may function distinctly in mice and humans; 2) UPF3A's role in NMD may have cell type specificity (Wallmeroth et al, 2022; Yi et al, 2022).

In this study, we used CRISPR-Cas9 technology and adopted the identical gene targeting strategy to generate a new *Upf3a* conditional knockout mouse strain. Furthermore, we characterized a newly released rabbit monoclonal antibody which could detect the expression of mouse UPF3A and UPF3B in a single immunoblotting (Supp Fig 1). With these key materials, we successfully produced and characterized *Upf3a* KO mESCs and somatic cells. We found that UPF3A and UPF3B protein expressions are higher in female ESCs than in male somatic cells (mouse rib muscle derived somatic cells) (Fig 1D), indicating that expressions of UPF3A and UPF3B proteins are developmentally regulated. Since undifferentiated female ESCs have two active Upf3b gene copies, while only one Upf3b gene locus is present in male RDSCs, the relative amount of UPF3B vs. UPF3A is reduced in male RDSCs.

In our study, we found that deletion of UPF3A was compatible with the life of embryonic stem cells and somatic cells, which was similar to UPF3B null mouse cells (Huang et al, 2011). Through qPCR and semi-quantitative RT-PCR assays, we found UPF3A loss did not cause decrease in mRNA transcripts of well-recognized NMD target genes. On the contrary, in *Upf3a* KO ESCs, somatic cells, as well as in various mouse tissues, including the liver and

thymus, transcript levels of these well-documented NMD targets remained unchanged or slightly upregulated. Of note, in *Upf3a* KO livers, mRNA transcripts of NMD target genes, including *Atf4*, *Snord22*, *Snhg12*, *1810032O08Rik and Hnrnpl* were mildly but significantly upregulated, indicating that UPF3A has tissue specificity in NMD. Thus, our study indicates that UPF3A is not a repressor of NMD. Our study, together with majority of previous studies on UPF3A and UPF3B, indicates that UPF3 paralogs are weak NMD activators in mammalian cells (Chan et al, 2009; Chan et al, 2007; Kunz et al, 2006; Lykke-Andersen et al, 2000; Wallmeroth et al, 2022; Yi et al, 2022). Furthermore, knockdown of UPF3B in UPF3A deficient ESCs causes evident NMD inhibition, which is in agreement with the previous hypothesis that UPF3B compensates for UPF3A loss and participates in NMD in mammalian cells.

Of note, in current study conducted with murine cells and tissues, to investigate the NMD efficacy, we only used qPCR and semi-quantitative RT-PCR assays and analyzed the expressions of 33 NMD targets with features of PTCs, uORFs or long 3' UTRs, which reveals UPF3A is dispensable for NMD in murine cells and tissues. However, we could not rule out the possibility that UPF3A may repress some un-characterized gene transcripts in certain unexplored mouse tissues, such as the testis with the highest UPF3A expression (Shum et al, 2016; Tarpey et al, 2007). Future transcriptome-wide analysis in *Upf3a* deficient murine cells or tissues would resolve UPF3A's role in NMD.

Materials and Methods

Mice and genotyping strategies

The *Upf3a* conditional knockout mouse (*Upf3a*$^{f/f}$) was generated by CRISPR–Cas9 gene editing in Cyagen. Cas9 protein, two gRNAs (gRNA1: AAATCTGTTGTTCGTACAGA, gRNA2: CTTGTTACAAGCTTTAGCCG) and a donor vector containing the two loxP sequences in intron 2 and intron 3 of mouse *Upf3a* gene were injected into mouse fertilized eggs. The embryos were transferred to recipient female mice to obtain F0 mice. For validating the two loxP site insertions, PCR products using two pairs of primers (F1: AAAGAACAGTGTGCAATTACTCGG, R1: TTCACAGGTAGGAACGATTCCATT; F2: TGTCCATTTTACCTATCCATTCG, R2: GAGCACTGCGCTACCACCTGACC) were sequenced. For routine genotyping of *Upf3a* alleles, three primers were used: F1, AAAGAACAGTGTGCAATTACTCGG; R1, TTCACAGGTAGGAACGATTCCATT; M1, AGCTCTTACTCTTGAGCCCAC (Wild-type allele: 133bps; Floxed allele: 200bps; knockout allele: 412bps) (Fig 1A). To generate the *Upf3a* inducible knockout mouse, *Upf3a*$^{f/f}$ mouse was crossed with Cre-ER^{T2+} transgenic mouse line. For genotyping of Cre-ER^{T2+} transgene, primers (Cre-ErF: ATACCGGAGATCATGCAAGC; Cre-ErR: GATCTCCACCATGCCCTCTA) were used (Cre-ER^{T2+} transgene: 552bps).

To delete *Upf3a* in adult *Upf3a*$^{f/f}$ Cre-ER^{T2+} mice (age: 6 weeks), tamoxifen (Sigma-Aldrich, T5648) was intraperitoneally injected at a dose of 75mg/kg for 3 consecutive days. Three weeks after the last tamoxifen injection, mice tissues were collected and processed for western blot and qPCR analysis.

All animals were maintained under specific pathogen-free conditions at the animal facility of the Shandong University, Qingdao, P. R. China. Animal care and experiments were performed in accordance with the ethic committee guideline.

Generation of UPF3A inducible deletion mESCs and somatic cells

mESC lines with *Upf3a* inducible deletion were generated and maintained by following a previously published protocol (Li et al, 2015). Briefly, *Upf3a*$^{f/f}$ Cre-ER^{T2+} males were crossed with *Upf3a*$^{f/f}$ Cre-ER^{T2-} females. At E3.5, blastocysts were flushed out with 1×D-PBS into 6cm sterile Petri-dish. Blastocysts were further transferred onto mitomycin C inactivated ICR MEF feeders. Around 5-7 days, once the inner cell masses/ESCs grew out of blastocysts, they were digested with 0.25% Trypsin and further cultured on feeders. The genotyping of the sex of each ESC line was conducted with published primers (Tunster, 2017).

Somatic cells from mouse rib muscle tissues (RDSCs) were generated with finely chopped rib muscle tissues from male *Upf3a*$^{f/f}$ Cre-ER^{T2+} mice at 4 weeks of age. The fine-chopped rib muscle tissues were attached to surfaces of 60mm cell culture dishes and cultured in EF medium (High Glucose DMEM, supplemented with 10% FBS, 100 units/ml Penicillin, and 100ug/ml Streptomycin). Around 5-7 days, when RDSCs grew out attached tissues, they were digested with 0.05% Trypsin and expanded in EF medium.

For the deletion of UPF3A in mESCs and RDSCs, 4-OHT (Sigma-Aldrich, H6278, 1uM) was used to treat cells for 5 successive days.

To measure the proliferation of ESCs, 1×10^6 ESCs were plated in 6-well plates precoated with 0.1% Gelatin. Numbers of ESCs were counted every 3 days.

Expressions of mouse UPF3A and UPF3B in U2OS cells

cDNAs of mouse *Upf3a* and *Upf3b* were amplified with PrimeSTAR® HS Premix (Takara) from an E14.1 ES cell cDNA library. The PCR products were further cloned in a pEGFP-C1-EF1a vector with a seamless cloning kit (D7010S，Beyotime) (Li et al, 2015). Sequences of pEGFP-C1-EF1a-mUpf3a and

pEGFP-C1-EF1a-mUpf3b were validated through sequencing services provided by Tsingke. These plasmids were amplified with E.Z.N. A® Endo-free plasmid Midi kit (Omega BIO-TEK) and transiently transfected into U2OS cells with Lipofectamine™ 3000 (Invitrogen) following the company protocols. Protein samples were harvested 48 hours after transfection.

Protein extraction and analysis

Cells or mouse tissues were lysed with RIPA buffer (Sigma-Aldrich, 20-188) supplemented with combinations of Protease/Phosphatase inhibitors (APExBIO). Around 40-60ug protein was separated with gradient SDS-PAGE gel (4-20%, ACE Biotechnology). The following primary antibodies were used: rabbit anti-UPF3A+UPF3B (ab269998, Abcam, 1:1000); mouse anti-β-Actin (A5441, Sigma-Aldrich, 1:10,000); mouse anti-Lamin B1 (sc-374015, Santa Cruz). The secondary antibodies used in these studies were HRP-conjugated goat anti-rabbit IgG or goat anti-mouse IgG (1:2,000; Proteintech).

qRT-PCR

Cells or mouse tissues were lysed with TRIzol Reagent (Sigma-Aldrich) and total RNAs were purified according to the company protocol. cDNAs were synthesized using HiScript® III 1st Strand cDNA Synthesis Kit (R312, Vazyme) according to the company manual. qRT-PCR in triplicate for each sample was performed using 2xTSINGKE® Master qPCR Mix (SYBR Green I) (TSINGKE) on the CFX96 Real-Time PCR system (Bio-Rad). The expression of β-Actin was used as the internal control.

Four sets of primers that amplify different parts of the *Upf3a* gene were used to quantify the *Upf3a* mRNA expression in control and *Upf3a* knockout ESCs. These primers are:

Upf3a-E1/E2: F, CCCTAAGTGAGAGCGGGG;

R, CTCTTCCAGCTGCTCTTTGG;

Upf3a-E2/E3: F, GCGCACGATTACTTCGAGGT;

R, TCAAAACGGTCTCTGAACAGC;

Upf3a-E7/E8: F, GTAAGAGGAAGGAGGCGGAG;

R, TTTCTCTGTGGCCACTTCCT;

Upf3a-E8/E9: F, TGGAGACGAGAAGCAGGAAG;

R, AGATCTCTTGTCCCTTGGCT.

To quantify the NMD efficiency with qPCR, 23 NMD target genes were selected: *Snhg12*, *Atf4*, *Gas5*, *1810032O08Rik*, and *Ddit3* (Weischenfeldt et al, 2008); *Cdh11*, *Ire1*, *Smad5*, *Smad7* and *Snord22* were retrieved from Shum *et al.* (Shum et al, 2016); *Auf1* and *Hnrnpl* were from Li et al (Li et al, 2015); *Eif4a2* (PTC isoform) was from Huth et al (Huth et al, 2022). Other gene-specific primers designed and used in this study are listed as bellow:

Smg5: F*, GGAACTGCTGTGGAGAAAGG;*

R, AGCGACCAGATGAGTCCTGT;

Smg6: F*,* GAGAACCCAGAGCAGATTCG;

R, CAAGCCCATCCATGTAGTCC;

Smg7: F, AACCCAAATCGAAGTGAAGTCC;

R, ACACCGTACACAGTTCCTGTAA;

Upf3b: F, AGGAGAAACGAGTGACCCTGT;

R, CCTGTTGCGATCCTGCCTA;

Eif4a1-PTC: F*, GGGTCGGACGCTCTATAAGT;*

R, GTCGGGGCCATTGTCTCT

Mettl23-PTC: F, ACCCAGCTCTTTCGGTTCC;

R, AGGAGGGATTAAGGGCATGG;

Sfrs10-PTC: F, TTCAGGAAAGGCCCGTAGC;

R, TGTCAAATGACGACTTCCGC;

Snrpb-PTC: F, AGAAGCCTCTGACCCTCTTCA;

R, GACCAGGTTCTCCCCTCGAA;

Hnrnpa2b1-PTC: F, GGTGGCTATGGTGGAAGGAG;

R, TACAGTCTTTGTGGCAGCAGA;

Luc7l-PTC: F, GGGAGTTGCAGAAAAGCCTC;

R, TGACTCTTGCAGACACGGTC;

Pkm2-PTC: F, CAGCGTGGAGGCCTCTTATA;

R, AAGTGGTAGATGGCAGCCTC.

For semi-quantitative RT-PCR analysis to identify the normal and the PTC^+ isoforms of *Pkm2*, *Rps9* and *Ptbp2*, primer sequences were retrieved from the previous study (Weischenfeldt et al, 2012). Primer sequences for *Eif4a2*, *Luc7l*, *Snrpb*, *Hnrnpa2b1*, *Sfrs10*, *Alkbh3*, *Sf1*, *Nfyb*, *Ccar1*, *Slc38a2* and *Flot1* were described previously (McIlwain et al, 2010).

Knockdown of *Upf3a* and *Upf3b* in mESCs

To knock down *Upf3a* and *Upf3b* in mESCs, control (non-target, NT-siRNA) (50pmol), mouse *Upf3a* siRNAs (50pmol) and *Upf3b* (50pmol) siRNAs were transfected by lipofectamine® RNAiMAX reagent (Invitrogen) into *Upf3a*-proficient and *Upf3a*-deficient mESCs with a previously published reverse transfection method (Li et al, 2015). The mESCs were maintained in the LIF-free differentiation condition. Twelve hours after the siRNA transfection, the medium was changed to the fresh ES medium and the cells were incubated for additional 48 hours. RNAi efficiency was investigated by qPCR and Western blotting around 60 hours after the siRNA transfection.

The following siRNA sequences are used:

Upf3a-1: 5’-AGAGAAACCCAAAGAAAGA-3’;

Upf3a-2: 5’-ACAGGATACCAGTGATAAA-3’;

Upf3a-3: 5’-GAGCACAAGGAGTATGACA-3’;

Upf3b-1: 5’-CCAAGAGACTGGACAAAGA-3’;

Upf3b-2: 5’-GCATGATCCGAGAAAGAGA-3’,

Upf3b-3: 5’- GAGTGAGAATACAGAATCA-3’.

All siRNAs are synthesized by RIBOBIO co. (Guangzhou, P. R. China).

Statistical analysis

The unpaired Student’s t-test was used in this study. The statistical analysis in this study was performed with GraphPad Prism (Ver 9.00, GraphPad Software, San Diego, CA, USA).

Acknowledgements

We thank all members of the Li laboratory for discussion and reading of the manuscript. We thank Dr. Haiyan Yu, Ms. Yuyu Guo and Ms. Xiaomin Zhao (Core Facilities for Life and Environmental Sciences, State Key laboratory of Microbial Technology, Shandong University) for helping with microscopy. Research projects in laboratory of Tangliang Li is supported by Grant No. LY22C050003, from the Natural Science Foundation of Zhejiang Province, China; Grants No. KF2020005 and KF2021008 from NHC Key Laboratory of Birth Defect for Research and Prevention (Hunan Provincial Maternal and Child Health Care Hospital, Changsha, China), Grant No. 31770871 from National Natural Science Foundation of China, and Qilu Youth Scholar Startup Funding of Shandong University.

Author contributions

C Chen: Investigation and data curation.

Y Shen: Investigation and data curation.

L Li: Investigation and data curation.

Y Ren: Resources.

Z-Q Wang: Resources.

T Li: Conceptualization, supervision, funding acquisition, manuscript writing.

Conflict of Interest Statement

The authors declare that they have no conflict of interest.

References:

Bufton JC, Powers KT, Szeto JA, Toelzer C, Berger I, Schaffitzel C (2022) Structures of

nonsense-mediated mrna decay factors upf3b and upf3a in complex with upf2 reveal molecular basis for competitive binding and for neurodevelopmental disorder-causing mutation. *Nucleic Acids Res* 50: 5934-5947. doi:10.1093/nar/gkac421

Chan WK, Bhalla AD, Le Hir H, Nguyen LS, Huang L, Gecz J, Wilkinson MF (2009) A upf3-mediated regulatory switch that maintains rna surveillance. *Nat Struct Mol Biol* 16: 747-753. doi:10.1038/nsmb.1612

Chan WK, Huang L, Gudikote JP, Chang YF, Imam JS, MacLean JA, 2nd, Wilkinson MF (2007) An alternative branch of the nonsense-mediated decay pathway. *Embo J* 26: 1820-1830. doi:10.1038/sj.emboj.7601628

Gao Z, Wilkinson M (2017) An rna decay factor wears a new coat: Upf3b modulates translation termination. *F1000Res* 6: 2159. doi:10.12688/f1000research.12704.1

Han X, Wei Y, Wang H, Wang F, Ju Z, Li T (2018) Nonsense-mediated mrna decay: A 'nonsense' pathway makes sense in stem cell biology. *Nucleic Acids Res* 46: 1038-1051. doi:10.1093/nar/gkx1272

Huang L, Lou CH, Chan W, Shum EY, Shao A, Stone E, Karam R, Song HW, Wilkinson MF (2011) Rna homeostasis governed by cell type-specific and branched feedback loops acting on nmd. *Mol Cell* 43: 950-961. doi:10.1016/j.molcel.2011.06.031

Huang L, Low A, Damle SS, Keenan MM, Kuntz S, Murray SF, Monia BP, Guo S (2018a) Antisense suppression of the nonsense mediated decay factor upf3b as a potential treatment for diseases caused by nonsense mutations. *Genome Biol* 19: 4. doi:10.1186/s13059-017-1386-9

Huang L, Shum EY, Jones SH, Lou CH, Dumdie J, Kim H, Roberts AJ, Jolly LA, Espinoza JL, Skarbrevik DM, et al (2018b) A upf3b-mutant mouse model with behavioral and neurogenesis defects. *Mol Psychiatr* 23: 1773-1786. doi:10.1038/mp.2017.173

Hug N, Longman D, Caceres JF (2016) Mechanism and regulation of the nonsense-mediated decay pathway. *Nucleic Acids Res* 44: 1483-1495. doi:10.1093/nar/gkw010

Huth M, Santini L, Galimberti E, Ramesmayer J, Titz-Teixeira F, Sehlke R, Oberhuemer M, Stummer S, Herzog V, Garmhausen M, et al (2022) Nmd is required for timely cell fate transitions by fine-tuning gene expression and regulating translation. *Genes Dev* 36: 348-367. doi:10.1101/gad.347690.120

Kunz JB, Neu-Yilik G, Hentze MW, Kulozik AE, Gehring NH (2006) Functions of hupf3a and hupf3b in nonsense-mediated mrna decay and translation. *RNA* 12: 1015-1022. doi:10.1261/rna.12506

Kurosaki T, Popp MW, Maquat LE (2019) Quality and quantity control of gene expression by nonsense-mediated mrna decay. *Nat Rev Mol Cell Bio* 20: 406-420. doi:10.1038/s41580-019-0126-2

Li T, Shi Y, Wang P, Guachalla LM, Sun B, Joerss T, Chen YS, Groth M, Krueger A, Platzer M, et al (2015) Smg6/est1 licenses embryonic stem cell differentiation via nonsense-mediated mrna decay. *EMBO J* 34: 1630-1647. doi:10.15252/embj.201489947

Lykke-Andersen J, Shu MD, Steitz JA (2000) Human upf proteins target an mrna for nonsense-mediated decay when bound downstream of a termination codon. *Cell* 103: 1121-1131. doi:10.1016/s0092-8674(00)00214-2

Lykke-Andersen S, Jensen TH (2015) Nonsense-mediated mrna decay: An intricate machinery that shapes transcriptomes. *Nat Rev Mol Cell Biol* 16: 665-677. doi:10.1038/nrm4063

Ma Z, Zhu P, Shi H, Guo L, Zhang Q, Chen Y, Chen S, Zhang Z, Peng J, Chen J (2019) Ptc-bearing mrna elicits a genetic compensation response via upf3a and compass components. *Nature* 568: 259-263. doi:10.1038/s41586-019-1057-y

McIlwain DR, Pan Q, Reilly PT, Elia AJ, McCracken S, Wakeham AC, Itie-Youten A, Blencowe BJ, Mak TW (2010) Smg1 is required for embryogenesis and regulates diverse genes via alternative splicing coupled to nonsense-mediated mrna decay. *Proc Natl Acad Sci U S A* 107: 12186-12191. doi:10.1073/pnas.1007336107

Neu-Yilik G, Raimondeau E, Eliseev B, Yeramala L, Amthor B, Deniaud A, Huard K, Kerschgens K, Hentze MW, Schaffitzel C, et al (2017) Dual function of upf3b in early and late translation termination. *EMBO J* 36: 2968-2986. doi:10.15252/embj.201797079

Serin G, Gersappe A, Black JD, Aronoff R, Maquat LE (2001) Identification and characterization of human orthologues to saccharomyces cerevisiae upf2 protein and upf3 protein (caenorhabditis elegans smg-4). *Mol Cell Biol* 21: 209-223. doi:10.1128/MCB.21.1.209-223.2001

Shum EY, Jones SH, Shao A, Dumdie J, Krause MD, Chan WK, Lou CH, Espinoza JL, Song HW, Phan MH, et al (2016) The antagonistic gene paralogs upf3a and upf3b govern nonsense-mediated rna decay. *Cell* 165: 382-395. doi:10.1016/j.cell.2016.02.046

Tarpey PS, Raymond FL, Nguyen LS, Rodriguez J, Hackett A, Vandeleur L, Smith R, Shoubridge C, Edkins S, Stevens C, et al (2007) Mutations in upf3b, a member of the nonsense-mediated mrna decay complex, cause syndromic and nonsyndromic mental retardation. *Nat Genet* 39: 1127-1133. doi:10.1038/ng2100

Tunster SJ (2017) Genetic sex determination of mice by simplex pcr. *Biol Sex Differ* 8: 31. doi:10.1186/s13293-017-0154-6

Wallmeroth D, Lackmann JW, Kueckelmann S, Altmuller J, Dieterich C, Boehm V, Gehring NH (2022) Human upf3a and upf3b enable fault-tolerant activation of nonsense-mediated mrna decay. *EMBO J* 41: e109191. doi:10.15252/embj.2021109191

Weischenfeldt J, Damgaard I, Bryder D, Theilgaard-Monch K, Thoren LA, Nielsen FC, Jacobsen SEW, Nerlov C, Porse BT (2008) Nmd is essential for hematopoietic stem and progenitor cells and for eliminating by-products of programmed DNA rearrangements. *Gene Dev* 22: 1381-1396. doi:10.1101/gad.468808

Weischenfeldt J, Waage J, Tian G, Zhao J, Damgaard I, Jakobsen JS, Kristiansen K, Krogh A, Wang J, Porse BT (2012) Mammalian tissues defective in nonsense-mediated mrna decay display highly aberrant splicing patterns. *Genome Biol* 13: R35. doi:10.1186/gb-2012-13-5-r35

Wittkopp N, Huntzinger E, Weiler C, Sauliere J, Schmidt S, Sonawane M, Izaurralde E (2009) Nonsense-mediated mrna decay effectors are essential for zebrafish embryonic development and survival. *Mol Cell Biol* 29: 3517-3528. doi:10.1128/Mcb.00177-09

Yi Z, Arvola RM, Myers S, Dilsavor CN, Abu Alhasan R, Carter BN, Patton RD, Bundschuh R, Singh G (2022) Mammalian upf3a and upf3b can activate nonsense-mediated mrna decay independently of their exon junction complex binding. *EMBO J* 41: e109202.

doi:10.15252/embj.2021109202
Yi Z, Sanjeev M, Singh G (2021) The branched nature of the nonsense-mediated mrna decay pathway. *Trends Genet* 37: 143-159. doi:10.1016/j.tig.2020.08.010

Figure legends

Figure 1. Generation of *Upf3a* knockout ESCs and somatic cells. (A) Strategy to generate *Upf3a* conditional knockout mouse. Exon 3 of *Upf3a* is chosen to be conditionally deleted by Cre recombinase *in vitro* and *in vivo*. Wild-type (wt) allele, floxed allele (F) and knockout allele (△) are shown. The locations of genotyping primers (F1, R1, and M1) are marked on these *Upf3a* alleles. **(B)** Mating strategy to generate *Upf3a* inducible knockout mouse line (*Upf3a*$^{f/f}$Cre-ER^{T2+}). *Upf3a*$^{f/f}$Cre-ER^{T2+} mice are further used to produce *Upf3a* inducible knockout embryonic stem cells (ESCs) and somatic cells from rib muscle (RDSCs). **(C)** PCR analysis on *Upf3a* locus (Exon 3) deletion in *Upf3a*$^{f/f}$Cre-ER^{T2+} ESCs and RDSCs after 4-OHT treatment. Wild-type allele (wt), floxed allele (F) and knockout allele (△) are marked. **(D)** Western blot analysis on UPF3A and UPF3B protein expression in *Upf3a*$^{f/f}$ Cre-ER^{T2+} ESCs and RDSCs after 4-OHT treatment. Protein lysates from U2OS cells expressing GFP-mUpf3a and GFP-mUpf3b are used to validate the UPF3A+UPF3B antibody. β-actin is used as a loading control for western blot. **(E)** Representative images of control ESCs/RDSCs (*Upf3a*$^{f/f}$) and *Upf3a* knockout (KO) ESCs/RDSCs (*Upf3a*$^{△/△}$).

Figure 2. UPF3A does not repress NMD targets expression.

(A-B) qPCR analysis on expressions of NMD targets in mESCs (**A**) and RDSCs **(B).** Due to considerable variances on expression levels of these NMD target genes between individual ESC and RDSC line, each data point (**A-B**) represents the relative expression of indicated gene in *Upf3a* KO related to its parental cell line. **(C-E)** qPCR analysis on expressions of NMD targets in liver **(C)**, thymus **(D)** and spleen **(E)** from control (Co, *Upf3a*$^{f/f}$Cre-ER^{T2-} + TAM) and *Upf3a* KO (*Upf3a*$^{△/△}$: *Upf3a*$^{f/f}$ Cre-ER^{T2+} + TAM) mice.

Note: *, P <0.05; ***, P <0.001; Unpaired Student's t-test is used.

Figure 3. RT-PCR analysis on AS-NMD in *Upf3a* KO ESCs (A, B) and RDSCs (C, D). Accumulations of PTC^+ isoforms generated with exon inclusion events (A, C) and exon skipping events (B, D) are analyzed by RT-PCR. ESC lines (ES1, ES2, ES3) and RDSC lines (M1, M3, M7) are used. Please note: AS-NMD defects in *Smg6* knockout (KO) ESCs and fibroblasts ($Smg6^{\triangle}$) are used as a positive control of NMD inhibition for this analysis.

Supplementary Figure legends

Supp Figure 1. UPF3A+UPF3B antibody characterization. (A) Predicted molecular weight of mouse UPF3A, UPF3B, and GFP tagged mouse UPF3A and UPF3B (GFP-mUpf3a and GFP-mUpf3b). **(B)** Western blot analysis on protein lysates from U2OS cells expressing GFP empty vector, GFP-mUpf3a and GFP-mUpf3b. A UPF3A+UPF3B antibody (Abcam 269998, 1:1000) is used to detected the fusion proteins (GFP-mUpf3a and GFP-mUpf3b). β-actin is used as a loading control for western blot. **(C)** Western blot analysis on protein lysates from ESC cells transfected with 3 siRNAs against mouse *Upf3a*, and 3 siRNAs against mouse *Upf3b*. Protein samples from untreated ESCs (Non transfection), RNAimax (reagent) treated ESCs, and non-targeting control (NC) siRNA treated ESCs are used as negative controls for *Upf3a* or *Upf3b* knockdown. β-actin is used as a loading control for western blot.

Supp Figure 2. Expression of truncated *Upf3a* mRNAs in *Upf3a* knockout ESCs and RDSCs. (A) The primer design strategy to detect different exons of mouse *Upf3a*. 3 pairs of qPCR primers to detect *Upf3a* exons 1-2 (fragment A), exons 7-8 (fragment B) and exons 8-9 (fragment C) are designed in this study. **(B)** qPCR analysis on different exon fragments of *Upf3a* mRNAs in ESCs and RDSCs. Relative expression between control (Co, *Upf3a*$^{f/f}$ CreER^{T2+}-OHT) and *Upf3a* KO (*Upf3a*$^{\Delta/\Delta}$, *Upf3a*$^{f/f}$ CreER^{T2+}+OHT) samples are shown.

Supp Figure 3. Generation and characterization of *Upf3a* KO ESCs and RDSCs. (A) Western blot analysis showed complete knockout of UPF3A in ESCs (Upper panel) and RDSCs (lower panel). Three independent ESC lines (ES1, ES2, ES3) and three independent RDSC lines (M1, M3, M7) are used for this analysis. **(B)** Proliferation of control (Co, *Upf3a*$^{f/f}$ CreER^{T2+}-OHT) and *Upf3a* KO (*Upf3a*$^{\Delta/\Delta}$, *Upf3a*$^{f/f}$ CreER^{T2+}+OHT) ESCs. ESCs derived from two

independent ESC lines (ES1 and ES2) are shown. For each passage, 1×10^6 ESCs are seeded in gelatin-coated 6-well dishes, and ESC numbers are counted every 3 days.

Supp Figure 4. NMD targets and their NMD inducing features.

Supp Figure 5. NMD inhibition in *Smg6* KO ESCs and fibroblasts. NMD target expressions in *Smg6* KO ESCs **(A)** and *Smg6* KO fibroblasts **(B)**. please note: Error bars represent the variance of technical replicates in qPCR assay.

Supp Figure 6. UPF3A is dispensable for NMD in ESCs. (A) Expressions of PTC containing isoforms of *Sfrs10*, *Snrpb*, *Hnrnpa2b1*, *Luc7l* and *Pkm2* in control (*Smg6*$^{F/F}$) and *Smg6* KO (*Smg6*$^{\Delta/\Delta}$) ESCs and fibroblasts. please note: Error bars represent the variance of technical replicates in qPCR assay. **(B)** Relative expressions of PTC containing isoforms of *Sfrs10*, *Snrpb*, *Hnrnpa2b1*, *Luc7l* and *Pkm2* in the *Upf3a* deficient (*Upf3a*$^{\Delta/\Delta}$) and control (*Upf3a*$^{f/f}$) ESCs and RDSCs. **(C)** Relative expressions of PTC containing isoforms of *Sfrs10*, *Snrpb*, *Hnrnpa2b1*, *Luc7l* and *Pkm2* in the *Upf3a* deficient (*Upf3a*$^{\Delta/\Delta}$) and control (*Upf3a*$^{f/f}$) spleen, thymus and liver samples.

Supp Figure 7. Co-depletions of UPF3A and UPF3B inhibit NMD in ESCs. Three siRNAs against mouse *Upf3b* are used to knockdown UPF3B expression in the control (Con, *Upf3a*$^{f/f}$ CreER^{T2+} -OHT) and *Upf3a* KO (*Upf3a*$^{\Delta/\Delta}$, *Upf3a*$^{f/f}$ CreER^{T2+} +OHT) ESCs. Semi-quantitative RT-PCR analysis on AS-NMD events in control (Con, *Upf3a*$^{f/f}$ CreER^{T2+} -OHT) and *Upf3a* KO (*Upf3a*$^{\Delta/\Delta}$, *Upf3a*$^{f/f}$ CreER^{T2+} +OHT) ESCs is shown. The *Smg6* KO ESC (Smg6$^{\Delta}$) is used as a positive control of AS-NMD inhibition. Two independent parental ESC lines with the genotype of *Upf3a*$^{f/f}$ CreER^{T2+} are used.

Note: RNAimax: reagent treatment; siRNA NC, non-targeting control siRNA treatment.

Supp Figure 8. Efficiencies of *Upf3a* deletion in TAM treated *Upf3a*$^{f/f}$ CreER^{T2+} mice. (A) PCR analysis of *Upf3a* gene locus in different organs from a male *Upf3a*$^{f/f}$ CreER^{T2+} mouse (21 days after Tamoxifen treatment). **(B)** Western blot analysis on UPF3A and UPF3B protein expression in the thymus, spleen, and liver from a pair of Tamoxifen treated male *Upf3a*$^{f/f}$ CreER^{T2-} and *Upf3a*$^{f/f}$ CreER^{T2+} mice.

Supp Figure 9. Semi-quantitative RT-PCR analysis on AS-NMD events in *Upf3a* KO livers (A, B) and spleens (C, D). Accumulations of PTC^{+} isoforms from exon inclusion (**A, C**) and exon skipping (**B, D**) are analyzed by RT-PCR. Please note: AS-NMD defects in *Smg6* KO ESC (Smg6$^{\Delta}$) are used as a positive control of NMD inhibition for this analysis.

Figure 1

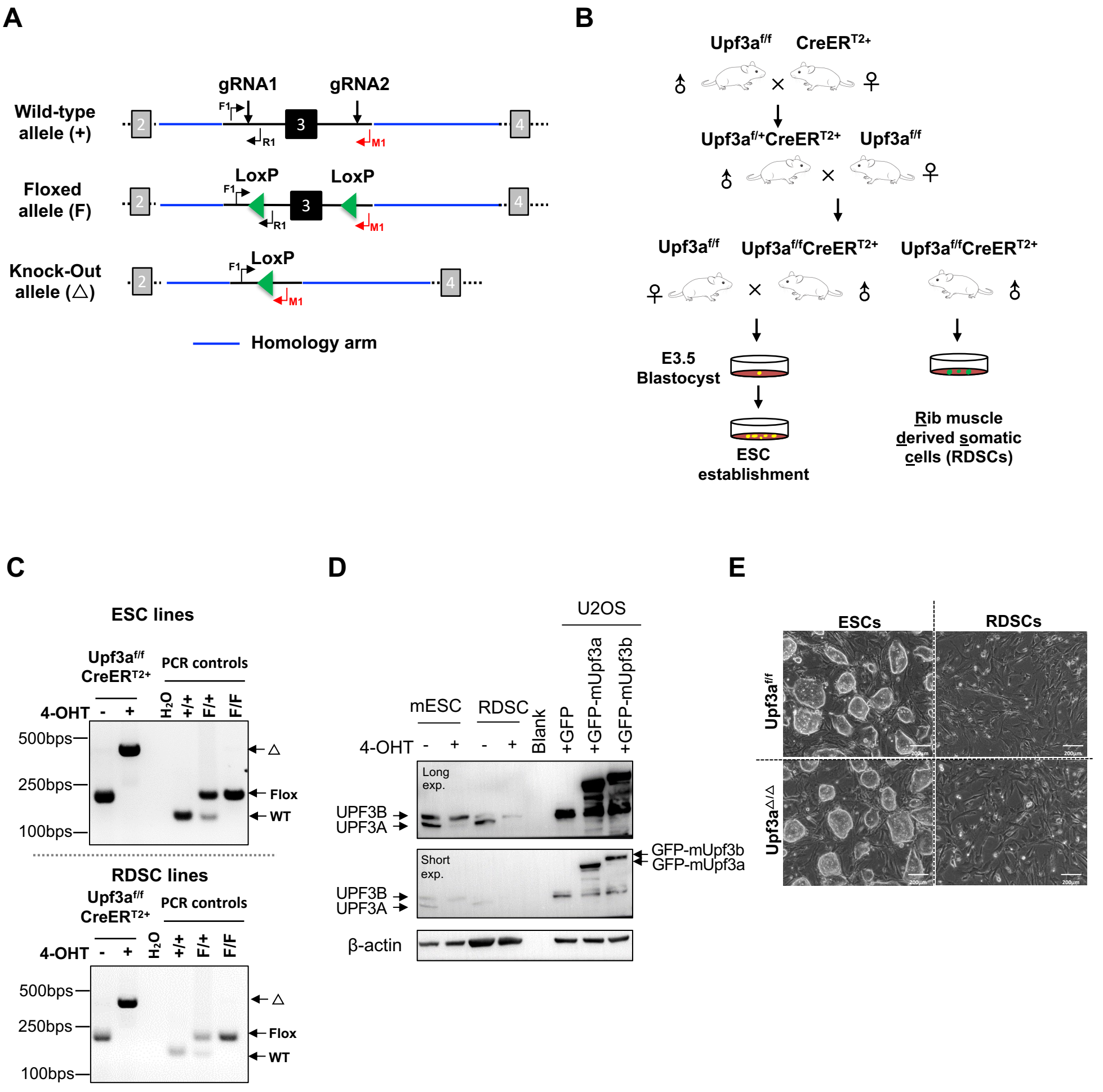
A
gRNA1
gRNA2
Wild-type allele (+)
Floxed allele (F)
Knock-Out allele (△)
LoxP
F1
R1
M1
Homology arm
B
Upf3a f/f
CreER T2+
Upf3a f/+ CreER T2+
Upf3a f/f CreER T2+
E3.5 Blastocyst
ESC establishment
Rib muscle derived somatic cells (RDSCs)
C
ESC lines
RDSC lines
PCR controls
4-OHT
H2O
+/+
F/+
F/F
500bps
250bps
100bps
Flox
WT
D
U2OS
mESC
RDSC
Blank
+GFP
+GFP-mUpf3a
+GFP-mUpf3b
Long exp.
Short exp.
UPF3B
UPF3A
GFP-mUpf3b
GFP-mUpf3a
β-actin
E
ESCs
RDSCs
Upf3a f/f
Upf3a △/△

Figure 2

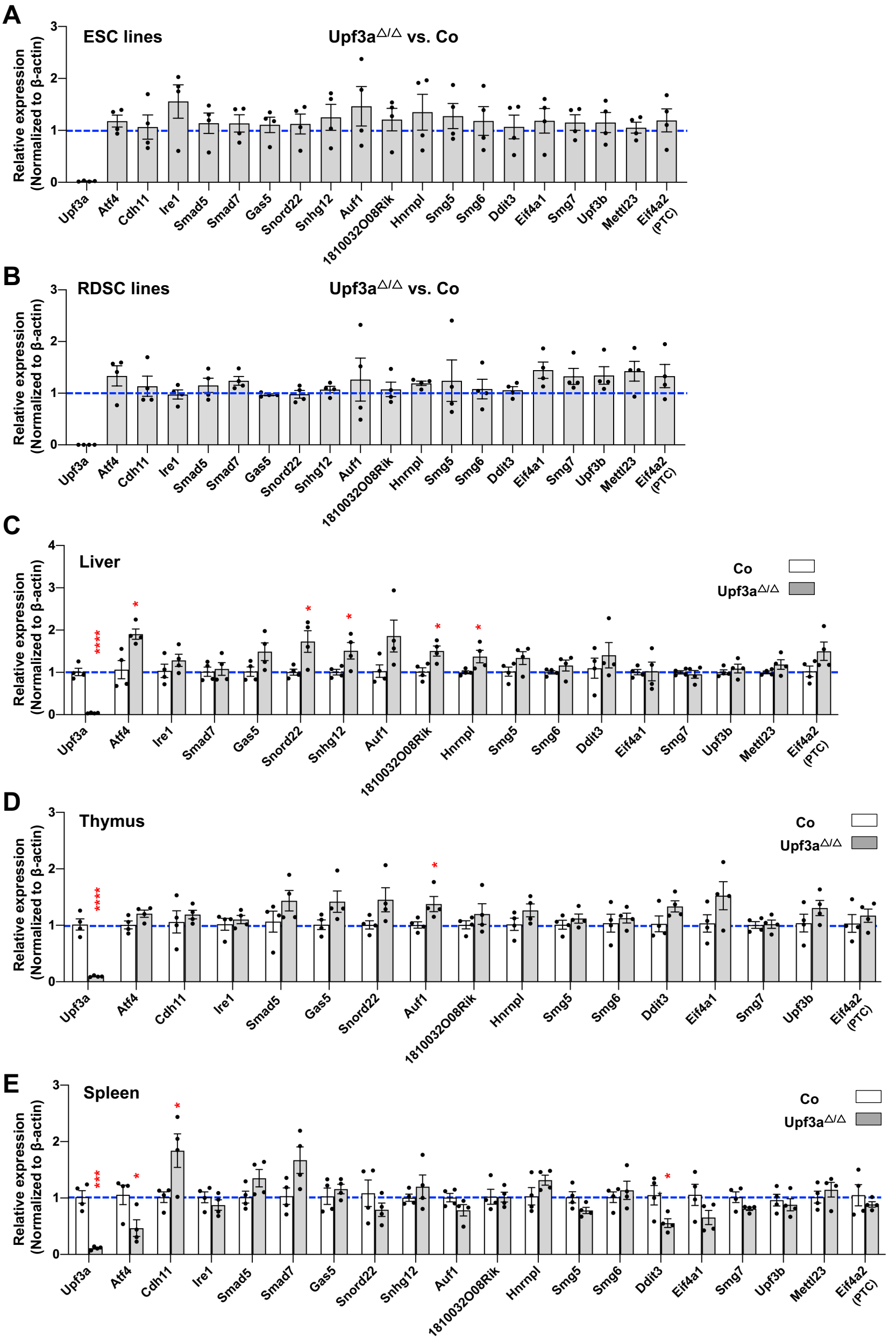
A
ESC lines
Upf3a△/△ vs. Co
Relative expression (Normalized to β-actin)
Upf3a
Atf4
Cdh11
Ire1
Smad5
Smad7
Gas5
Snord22
Snhg12
Auf1
1810032O08Rik
Hnrnpl
Smg5
Smg6
Ddit3
Eif4a1
Smg7
Upf3b
Mettl23
Eif4a2 (PTC)
B
RDSC lines
Upf3a△/△ vs. Co
C
Liver
Co
Upf3a△/△
D
Thymus
E
Spleen

Figure 3

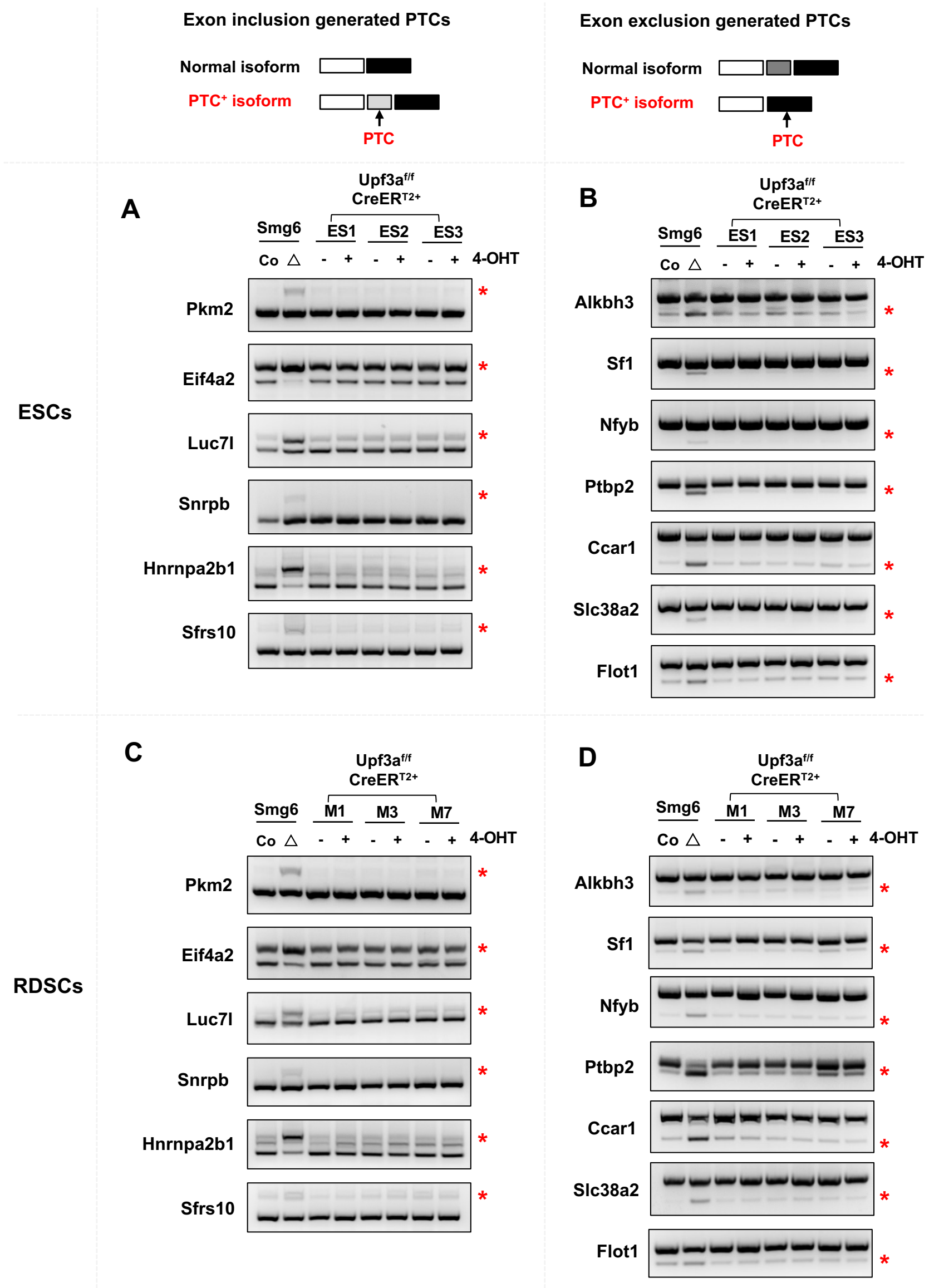
Exon inclusion generated PTCs
Normal isoform
PTC+ isoform
PTC
Exon exclusion generated PTCs
Normal isoform
PTC+ isoform
PTC
ESCs
A
Upf3af/f
CreERT2+
Smg6
ES1
ES2
ES3
Co △ - + - + - + 4-OHT
Pkm2
Eif4a2
Luc7l
Snrpb
Hnrnpa2b1
Sfrs10
B
Upf3af/f
CreERT2+
Smg6
ES1
ES2
ES3
Co △ - + - + - + 4-OHT
Alkbh3
Sf1
Nfyb
Ptbp2
Ccar1
Slc38a2
Flot1
RDSCs
C
Upf3af/f
CreERT2+
Smg6
M1
M3
M7
Co △ - + - + - + 4-OHT
Pkm2
Eif4a2
Luc7l
Snrpb
Hnrnpa2b1
Sfrs10
D
Upf3af/f
CreERT2+
Smg6
M1
M3
M7
Co △ - + - + - + 4-OHT
Alkbh3
Sf1
Nfyb
Ptbp2
Ccar1
Slc38a2
Flot1